NASA/TM—2002-211982

Experimental Evaluation of a Subscale Gaseous Hydrogen/Gaseous Oxygen Coaxial Rocket Injector

Timothy D. Smith, Mark D. Klem, and Kevin J. Breisacher
Glenn Research Center, Cleveland, Ohio

Shahram Farhangi and Robert Sutton
Boeing, Rocketdyne Division, Canoga Park, California

November 2002

The NASA STI Program Office . . . in Profile

Since its founding, NASA has been dedicated to the advancement of aeronautics and space science. The NASA Scientific and Technical Information (STI) Program Office plays a key part in helping NASA maintain this important role.

The NASA STI Program Office is operated by Langley Research Center, the Lead Center for NASA's scientific and technical information. The NASA STI Program Office provides access to the NASA STI Database, the largest collection of aeronautical and space science STI in the world. The Program Office is also NASA's institutional mechanism for disseminating the results of its research and development activities. These results are published by NASA in the NASA STI Report Series, which includes the following report types:

- TECHNICAL PUBLICATION. Reports of completed research or a major significant phase of research that present the results of NASA programs and include extensive data or theoretical analysis. Includes compilations of significant scientific and technical data and information deemed to be of continuing reference value. NASA's counterpart of peer-reviewed formal professional papers but has less stringent limitations on manuscript length and extent of graphic presentations.

- TECHNICAL MEMORANDUM. Scientific and technical findings that are preliminary or of specialized interest, e.g., quick release reports, working papers, and bibliographies that contain minimal annotation. Does not contain extensive analysis.

- CONTRACTOR REPORT. Scientific and technical findings by NASA-sponsored contractors and grantees.

- CONFERENCE PUBLICATION. Collected papers from scientific and technical conferences, symposia, seminars, or other meetings sponsored or cosponsored by NASA.

- SPECIAL PUBLICATION. Scientific, technical, or historical information from NASA programs, projects, and missions, often concerned with subjects having substantial public interest.

- TECHNICAL TRANSLATION. English-language translations of foreign scientific and technical material pertinent to NASA's mission.

Specialized services that complement the STI Program Office's diverse offerings include creating custom thesauri, building customized databases, organizing and publishing research results . . . even providing videos.

For more information about the NASA STI Program Office, see the following:

- Access the NASA STI Program Home Page at ***http://www.sti.nasa.gov***

- E-mail your question via the Internet to help@sti.nasa.gov

- Fax your question to the NASA Access Help Desk at 301–621–0134

- Telephone the NASA Access Help Desk at 301–621–0390

- Write to:
  NASA Access Help Desk
  NASA Center for AeroSpace Information
  7121 Standard Drive
  Hanover, MD 21076

NASA/TM—2002-211982

Experimental Evaluation of a Subscale Gaseous Hydrogen/Gaseous Oxygen Coaxial Rocket Injector

Timothy D. Smith, Mark D. Klem, and Kevin J. Breisacher
Glenn Research Center, Cleveland, Ohio

Shahram Farhangi and Robert Sutton
Boeing, Rocketdyne Division, Canoga Park, California

National Aeronautics and
Space Administration

Glenn Research Center

November 2002

Available from

NASA Center for Aerospace Information
7121 Standard Drive
Hanover, MD 21076

National Technical Information Service
5285 Port Royal Road
Springfield, VA 22100

Available electronically at http://gltrs.grc.nasa.gov

Experimental Evaluation of a Subscale Gaseous Hydrogen / Gaseous Oxygen Coaxial Rocket Injector

Timothy D. Smith
Mark Klem
Kevin J. Breisacher
National Aeronautics and Space Administration
Glenn Research Center
Cleveland, Ohio 44135

Shahram Farhangi
Robert Sutton
Boeing Rocketdyne Division
Canoga Park, California

Abstract

The next generation reusable launch vehicle may utilize a Full-Flow Stage Combustion (FFSC) rocket engine cycle. One of the key technologies required is the development of an injector that uses gaseous oxygen and gaseous hydrogen as propellants. Gas-gas propellant injection provides an engine with increased stability margin over a range of throttle set points. This paper summarizes an injector design and testing effort that evaluated a coaxial rocket injector for use with gaseous oxygen and gaseous hydrogen propellants. A total of 19 hot-fire tests were conducted up to a chamber pressure of 1030 psia, over a range of 3.3 to 6.7 for injector element mixture ratio. Post-test condition of the hardware was also used to assess injector face cooling. Results show that high combustion performance levels could be achieved with gas-gas propellants and there were no problems with excessive face heating for the conditions tested.

Symbols

A	Area, in^2
Cp	specific heat based upon constant pressure, BTU/lb_m-°R
C*	characteristic exhaust velocity, ft/s
C^*_{EXP}	experimental characteristic exhaust velocity, ft/s
C^*_{MA}	calculated mass average characteristic exhaust velocity, ft/s
$C^*_{Th(x)}$	theoretical, one-dimensional characteristic exhaust velocity obtained from the CEA program, ft/s
g	proportionality constant (32.2 lb_m-ft/lb_f-s)
h	enthalpy, BTU/lb_m
K_c	empirical injector design function, dimensionless
m	propellant mass flow, lb_m/s
m_T	total propellant mass flow, lb_m/s
MRT	injector inlet momentum ratio (fuel divided by oxidizer), dimensionless
O/F	propellant mixture ratio (oxidizer flow divided by fuel flow), dimensionless
Pc	combustion chamber pressure, psia
R	gas constant, lb_f-ft/lb_m-°R
T	propellant temperature, °R

V	Velocity, ft/s
VR	injector inlet velocity ratio (fuel divided by oxidizer), dimensionless
η_{C*}	characteristic exhaust velocity efficiency, percent
γ	ratio of specific heats
ρ	density, lb_m/in^3

Subscripts

BLC	boundary layer hydrogen
C	injector core flow
H_2	hydrogen
O_2	oxygen
t	rocket throat
T	results based on total massflow

Background

The Full-Flow Stage Combustion (FFSC) rocket engine cycle continues to be a promising system for the next generation of space launch vehicles. The FFSC cycle provides the potential for increased specific impulse efficiency over a wide range of power settings due to improved throttling stability margin. The improved stability margins result from the use of gaseous propellants, which provide consistent pressure drop ratios above stability criteria levels. More importantly, the FFSC cycle can improve engine reliability and reduce complexity. The key to the cycle is the use of both fuel-rich and oxidizer-rich gases to power the fuel and oxidizer turbopumps respectively.[1] Turbine inlet temperatures are lowered because all of the propellants are routed through preburners to power the turbomachinery. This is unlike other systems, such as fuel rich staged combustion, where the turbomachinery is primarily driven by the amount of fuel flow. The FFSC cycle also reduces system complexity by eliminating the need for inner propellant seals on the oxygen turbopump.

One of the key components to the performance of a FFSC rocket engine is the main injector. A first look would indicate that the development of gaseous hydrogen-gaseous oxygen injectors would be a straightforward process when compared to liquid systems. The elimination of atomization and vaporization from the combustion process should dramatically simplify the design process. However, as with any rocket component development, this type of injector has its own unique set of design challenges. As discussed in reference 2, propellant mixing is a critical driver to development of gas-gas injectors. Not only does propellant mixing drive the performance level, it also has a significant impact on face cooling and injector durability.

Over the years work has been carried out to investigate the use of gaseous propellants for main injectors[2345]. The bulk of work has been focused on the investigation of gaseous hydrogen and liquid oxygen. However, that work scale has been on small thrusters for on orbit applications, not large-scale launch engines. Aerojet performed a comprehensive study[6] of gas-gas rocket injectors under NASA contract in the 1970's. The program evaluated a wide-range of both single- and multi-element injector configurations in both cold-flow and hot-fire tests. The results also include a design guide based upon the empirical results. However, much of the data was generated for smaller scale elements, which operated at lower flowrates and pressures than those required by current FFSC systems.

The search for the next generation of reusable launch vehicles has refocused efforts to examining the use of the FFSC. To address the need for further development of gas-gas injectors, NASA initiated a cooperative effort between government, industry, and academia to investigate injector element concepts[7]. As part of this program, both single-element and multi-element testing was conducted on a variety of injector concepts. Single element testing was used to obtain species measurements using Raman laser techniques[8]. Results from that project further enhanced the database by providing multi-element data at chamber pressures up to 1200 psia.

The objective of the current gas-gas injector test program is to build upon the previous results and examine the performance of a coaxial injector during hot-fire. Testing was conducted with a multi-element injector up to a chamber pressure of 1050 psia using ambient temperature hydrogen and oxygen. Pressure and temperature measurements were used to determine combustion performance. Post-test condition of the hardware was also used to address injector face cooling.

Test Facility

Testing was conducted in Cell 32 of the Research Combustion Laboratory[9]. The cell is part of a highly flexible facility that encompasses several test cells for both combustion research and material evaluation. Cell 32 is capable of testing with a variety of propellants including gaseous oxygen and gaseous hydrogen, liquid oxygen and liquid hydrogen, and hydrocarbon propellants. A 1500 psia water system is also available for combustor cooling applications. The facility can accommodate combustors that generate thrust levels up to 2000 lb_f with chamber pressures to 1200 psia. The propellant systems consisted of a gaseous oxygen circuit and a gaseous hydrogen circuit fed from 2400 psia roadable tube trailers. The gaseous hydrogen circuit was split into two legs inside of the test cell to supply both the main propellant and boundary layer cooling propellant. Each propellant circuit used calibrated subsonic venturis for flow measurement.

Test Hardware

Rocketdyne, as part of a cooperative test program, provided the combustion chamber, including injector, window, and nozzle housings. Figure 1 shows a test firing with the windows installed during a previous program.

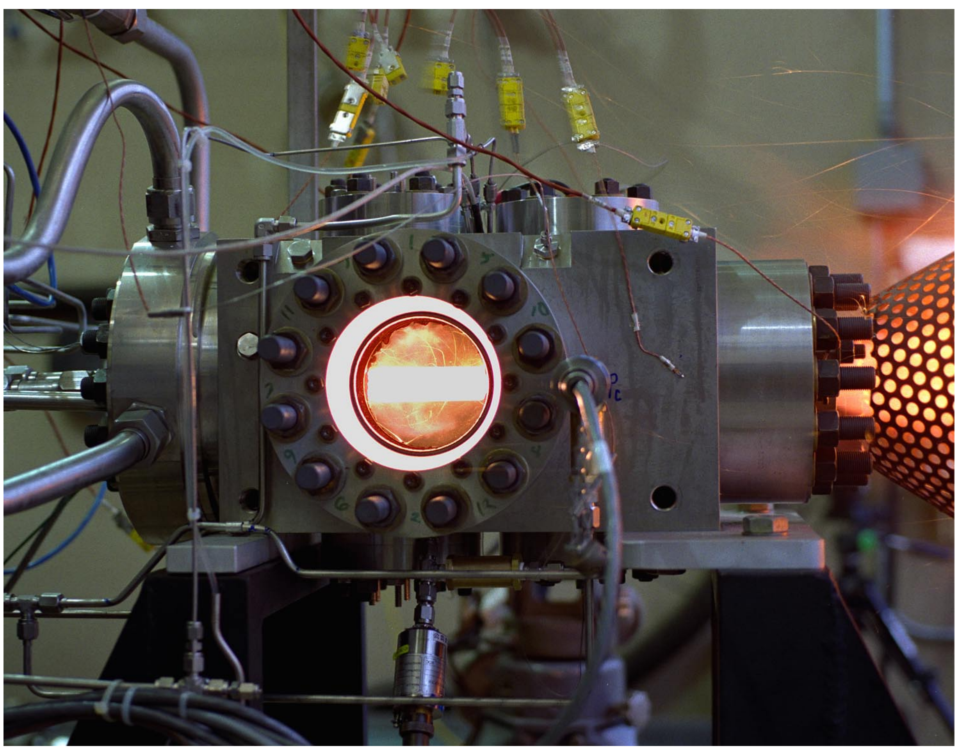

Figure 1.—Test firing of heat sink combustion chamber with optical access windows.

The combustion chamber is a heat sink configuration made of stainless steel with zirconia coated nozzle inserts. It can be observed in the photograph that there is significant thermal mass available for heat dissipation. Table 1 provides the relevant dimensions for the test configuration.

TABLE 1.—COMBUSTION CHAMBER DIMENSIONS

	Dimension
Chamber diameter, in.	4.00
Throat diameter, in.	1.18
Contraction ratio	11.49
Exit diameter, in.	1.84
Exit area ratio	2.42
Chamber length, in.	10.60

The hardware consists of a number of interchangeable parts that can be modified depending upon the test requirements. As shown in figure 2, the hardware can accommodate two large side windows for optical access along with four smaller windows on the top and bottom for optical access.

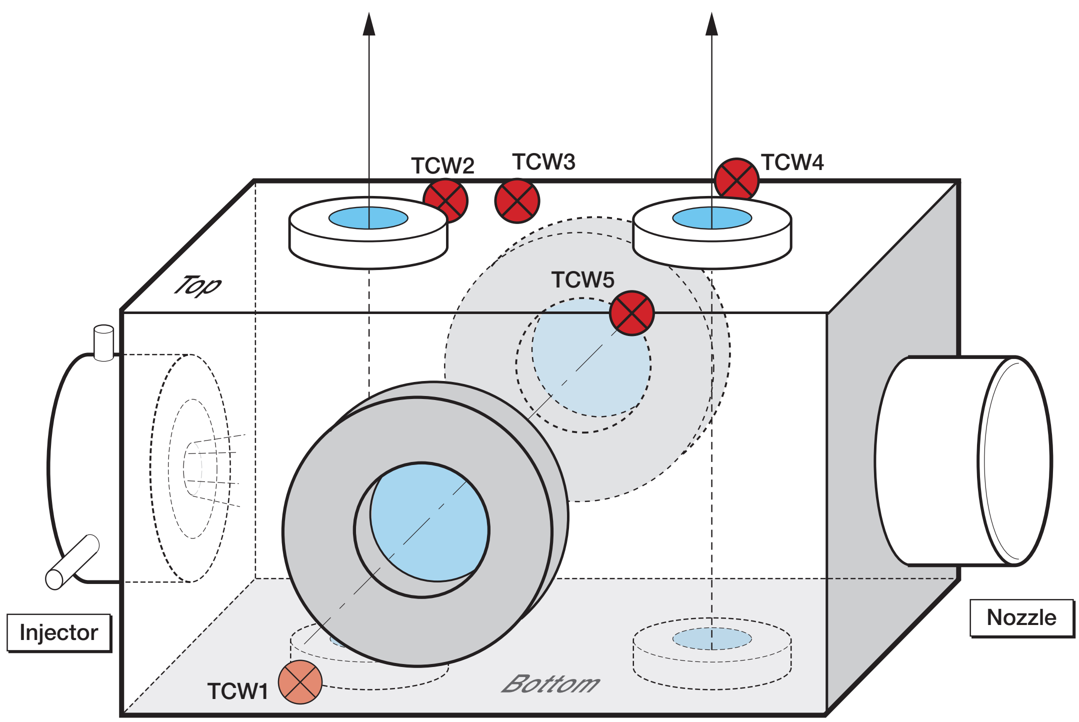

Figure 2.—Schematic of heat sink combustion chamber assembly.

Ignition was provided by a spark plug located in the top, downstream window location. The combustion chamber nozzle consisted of two parts, the main nozzle housing which attached to the chamber body, and a smaller throat insert. The throat insert could be varied to provide a wide variety of throat diameters. The injector consisted of two parts: a main housing and an injector insert. The injector housing was recessed into the combustion chamber so the injector face plane was just upstream of the large side windows. Oxygen was fed to the injector through a single line located straight back from the center of the injector face. Both main and boundary layer hydrogen were fed through multiple feed lines to provide even distribution around the face. The modular design of the combustion chamber provides a high level of flexibility for injector evaluation.

As stated previously, there is no large database to use when designing or analyzing gas-gas rocket engine injectors. To initiate the design, ground rules were established based on facility pressure, thrust, and flow rate limits. Nominal design was based upon a chamber pressure of 1000 psia at a mixture ratio of six. The designs were compared to the gas-gas injector design procedure found in reference 7. However, since that work was at low chamber pressures this analysis can be considered an extrapolation. The two parameters of interest, based on reference 7, are the mixing efficiency and the energy release efficiency. Following the design procedure, the mixing efficiency was estimated to be 90.5 percent and the energy release efficiency to be above 99 percent for the current design.

The injector tested during this effort was a seven-element shear coaxial design with oxygen fed though the main post and hydrogen through the surrounding annulus. Figure 3 is a pretest photograph of the multi-element injector.

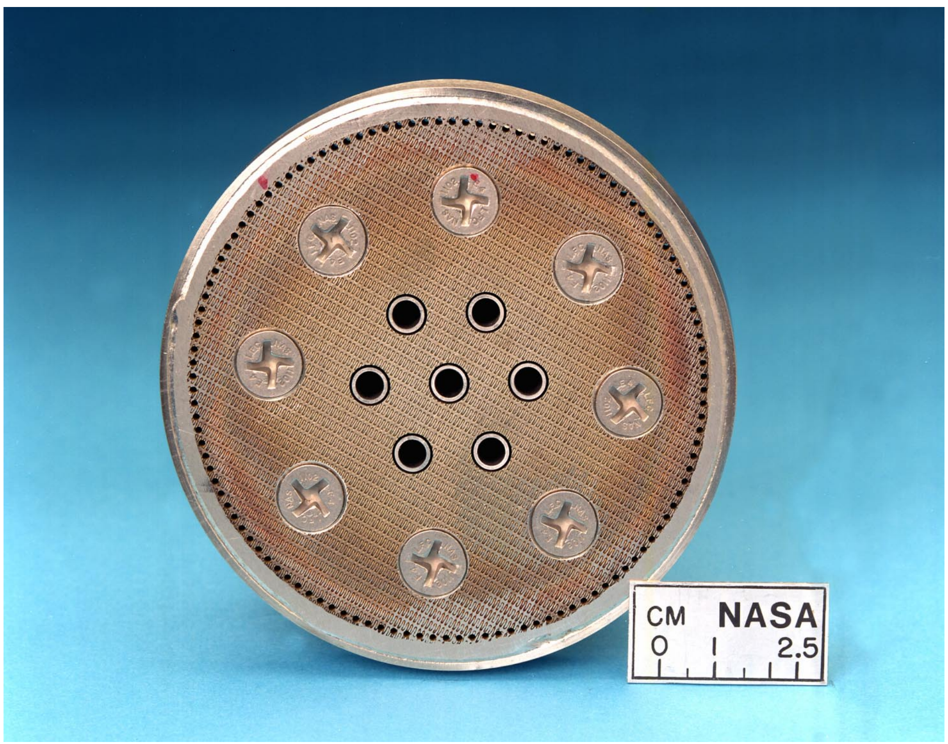

Figure 3.—Gas-gas coaxial injector with boundary layer cooling orifices.

The main injector design had a single element located in the center and 6 elements equally spaced on a diameter of 1.1 in. The oxygen posts were 0.197-in. diameter, with a 0.025-in. wall thickness. Hydrogen was injected through a straight, 0.0175-in. annular gap around the oxygen post. A porous sintered wire mesh faceplate was used to provide face cooling. Boundary layer cooling (BLC) was provided through the 120, 0.050-in. diameter cooling jets located along the outer face diameter. The boundary layer coolant and main hydrogen propellant circuits were fed and measured separately. A plate is located behind the face, at the same diameter as the face screws, to keep the gas supplies from mixing. As with the combustion chamber, the part was manufactured from stainless steel.

Figure 4 is a schematic showing propellant feed system to the hardware along with instrumentation locations.

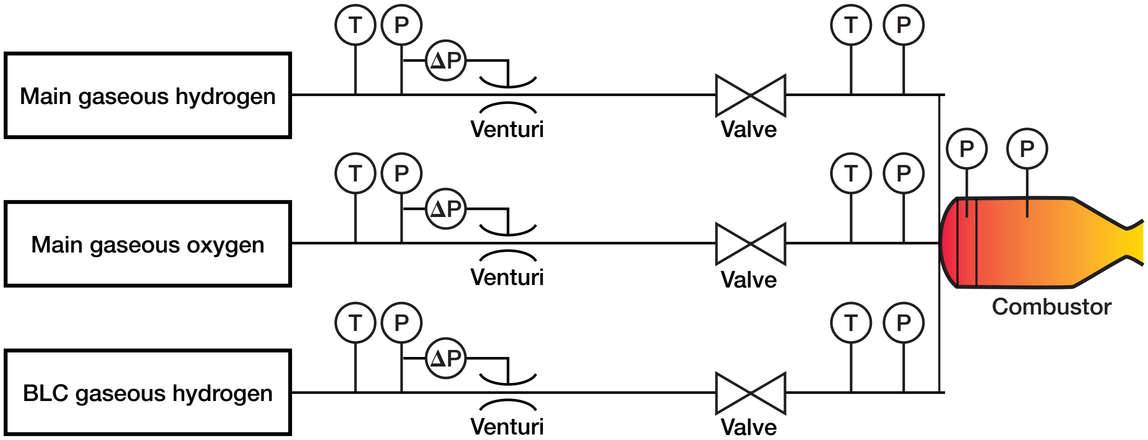

Figure 4.—Schematic showing propellant circuits and instrumentation.

Redundant pressure and temperature measurements were made at the injector inlet connections to the feed lines on each circuit. Chamber pressure was measured at two axial locations, 1.9-in. and 7.4-in. downstream of the injector face. The measurements were separated radially by approximately 90 degrees. The combustion chamber also could accommodate a variety of thermocouple measurement locations. For this test series, five locations (figure 2) were used to measure gas temperature along the internal wall of the combustion chamber. Each thermocouple was mounted such that the tip was slightly into the combustion zone. The location of the thermocouples is described in table 2.

TABLE 2.—COMBUSTION CHAMBER THERMOCOUPLE LOCATIONS

Thermocouple	Axial location, in.	Radial location, deg
TCW1	1.9	152.5
TCW2	1.9	27.5
TCW3	3.4	27.5
TCW4	5.5	45
TCW5	5.5	315

Experimental Results

Performance

A total of 19 hot-fire tests were completed with the coaxial injector design over a range of chamber pressure and mixture ratio conditions. All propellants were injected at ambient temperature (529 to 555 °R). The injector survived the testing with no significant discoloration or erosion to either the faceplate or oxygen posts.

The key values measured for each run were chamber pressure, propellant flowrates, and combustion chamber wall temperatures. The target mixture ratio levels were based upon injector element (core) mixture ratio as opposed to total mixture ratio, which includes the boundary layer coolant. These parameters were defined by the following:

$$\left(\frac{O}{F}\right)_T = \frac{\dot{m}_{O_2}}{\dot{m}_{H_2} + \dot{m}_{BLC}} \qquad \textbf{(1)}$$

$$\left(\frac{O}{F}\right)_C = \frac{\dot{m}_{O_2}}{\dot{m}_{H_2}} \quad \textbf{(2)}$$

For the current series of tests, the main figure of merit for injector performance is characteristic exhaust velocity (C^*_{EXP}). By definition,

$$C^*_{EXP} = \frac{PcA_t g}{\dot{m}} \quad \textbf{(3)}$$

To obtain C* efficiency, the calculated C^*_{EXP} values were divided by the theoretical, one-dimensional-equilibrium values obtained from the Chemical Equilibrium Composition and Applications[10] (CEA) program. Inputs to the CEA code included chamber pressure, mixture ratio, chamber contraction ratio, and propellant inlet temperature. Propellant inlet temperatures were input so the code could calculate the corresponding inlet enthalpy. The characteristic exhaust velocity efficiency is defined as:

$$\eta_{C^*} = \frac{C^*_{EXP}}{C^*_{Th(ODE)}} \quad \textbf{(4)}$$

Due to the abundance of boundary layer cooling present in the system, it is difficult to determine the true performance of the injection elements. The flow within the combustion chamber could vary between fully mixed and completely stratified, where the core and boundary layer stay in streamtubes. To examine the differences in performance, three sets of analysis were conducted to bound the performance range. The analysis was conducted based on the assumption of fully mixed flow, core flow with ambient temperature boundary layer cooling flow, and core flow with 2000 °R boundary layer cooling flow.

For the analysis of the fully mixed conditions, combustion performance was based upon measured chamber pressure and total mixture ratio. This analysis assumes complete mixing between the core flow from the injector elements and the boundary layer coolant. The input values to CEA for mixture ratio would be from equation 1 and combustion performance calculated from equations 3 and 4.

The stratified flow analysis breaks the flow up into two streamtubes, one based on the core flow from the injector, and the other a boundary layer flow of pure hydrogen at specified temperatures. The theoretical C* values must be calculated for each streamtube. The hydrogen boundary layer C* can be calculated from the following equation based upon the assumed temperature (T_{BLC}), gas constant (°R), and ratio of specific heats (γ).

$$C^*_{BLC} = \frac{\sqrt{g\gamma R_{H_2} T_{BLC}}}{\gamma\sqrt{\left[\frac{2}{\gamma+1}\right]^{\frac{\gamma+1}{\gamma-1}}}} \quad \textbf{(5)}$$

For hydrogen the gas constant is 766.4 ft-lb_f/lb_m-°R and the ratio of specific heats is 1.4. From equation 5, for a 2000 °R hydrogen boundary layer the C* is 10 253 ft/s and over the range of ambient inlet temperatures is 5270 to 5405 ft/s. The core C* is calculated from the CEA program based upon the measured chamber pressure and mixture ratio through the injector elements (equation 2).

A new theoretical C* is then calculated on a mass average basis from the core C* and the boundary layer C*. For the case where the boundary layer streamtube was at ambient temperature, there is no heat transfer assumed from the core flow. However, for the case where streamtube flow is heated to 2000 °R, heat must be transferred from the core flow to the boundary layer flow. The amount of heat transferred from the core flow to the boundary layer can be determined by calculating the change in enthalpy required to raise the incoming hydrogen flow to 2000 °R.

$$\Delta h_{BLC} = Cp_{BLC}\left(2000 - T_{H_2 Inlet}\right) = -\Delta h_C \tag{6}$$

The new core C* was calculated from CEA by adjusting the inlet enthalpy of the hydrogen based upon the reduced core enthalpy calculated from equation 6.

$$C^*_{Th,MA} = \frac{\dot{m}_C}{\dot{m}_T} C^*_{Th(C)} + \frac{\dot{m}_{BLC}}{\dot{m}_T} C^*_{BLC} \tag{7}$$

Combustion efficiency for the stratified flow cases can then be calculated by modifying equation 6 as follows:

$$\eta_{C^*_{MA}} = \frac{C^*_{Exp}}{C^*_{Th,MA}} \tag{8}$$

Table 3 presents a summary of the conditions, flowrates, and results for the test series.

TABLE 3.—HOT-FIRE TEST RESULTS FOR GASEOUS HYDROGEN / GASEOUS OXYGEN COAXIAL INJECTOR

RDG	Chamber pressure, psia	Total mixture ratio	Injector mixture ratio	Oxygen flow, lb_m/s	Injector H_2 flow, lb_m/s	BLC H_2 flow, lb_m/s	η_{C^*} mixed, percent	η_{C^*} T_{BLC}=Amb., percent	η_{C^*} T_{BLC}=2000 °R, percent
1	513.0	1.39	6.15	1.31	0.21	0.73	98.4	115.8	103.9
2	513.6	1.40	6.21	1.33	0.21	0.73	97.4	114.9	104.1
3	471.1	0.96	3.67	1.02	0.28	0.79	101.2	110.8	106.4
4	587.6	1.39	5.35	1.48	0.28	0.79	99.1	114.1	105.4
5	471.4	0.97	3.77	1.03	0.27	0.78	101.0	111.1	106.4
6	464.2	1.12	5.81	1.08	0.19	0.78	100.1	117.1	106.7
7	712.1	1.28	3.43	1.71	0.50	0.84	101.3	109.5	105.2
8	707.8	1.26	3.29	1.70	0.52	0.83	100.9	108.6	104.6
9	712.3	1.48	4.68	1.83	0.39	0.84	99.7	111.8	105.0
10	752.6	1.80	6.03	2.08	0.34	0.81	98.5	115.1	106.1
11	749.2	1.80	5.99	2.07	0.34	0.80	98.5	115.0	106.0
12	866.8	1.66	3.61	2.28	0.63	0.74	100.9	108.4	104.5
13	899.7	1.37	3.63	2.23	0.61	1.01	100.6	109.2	104.5
14	898.8	1.39	3.68	2.24	0.61	1.00	100.6	109.3	104.6
15	952.4	1.91	6.74	2.71	0.40	1.01	97.6	116.4	106.4
16	917.7	1.80	6.34	2.54	0.40	1.01	98.3	115.9	106.2
17	1030.3	1.86	4.89	2.84	0.58	0.94	99.7	111.3	105.2
18	1022.1	1.97	5.34	2.88	0.54	0.93	99.2	112.3	105.4
19	1000.1	2.03	6.39	2.88	0.45	0.97	97.8	114.9	106.0

From table 3 it is apparent that combustion performance varied over the range of conditions tested. The C* efficiency for the fully mixed values greater than 100 percent can be attributed to uncertainty in the measured data. An uncertainty analysis was conducted for the tests completed based upon the method described in reference 12. Results from the analysis show an uncertainty range of 4 to 6 percent for C* efficiency. Therefore, it is best to view the performance results in terms of general trends as opposed to a quantitative assessment. The streamtube calculation methods are significantly higher than 100 percent efficiency, which indicates that the propellants were mixing well before the chamber throat and thus the fully mixed analysis is the best measure to evaluate trends in the data. Clearly the assumption of an ambient temperature boundary layer flow is not physically relevant for this type of system. However, it was felt the analysis would provide an interesting point of comparison with the other methods. Figure 5 presents C* efficiency for each calculation method as a function of total mixture ratio.

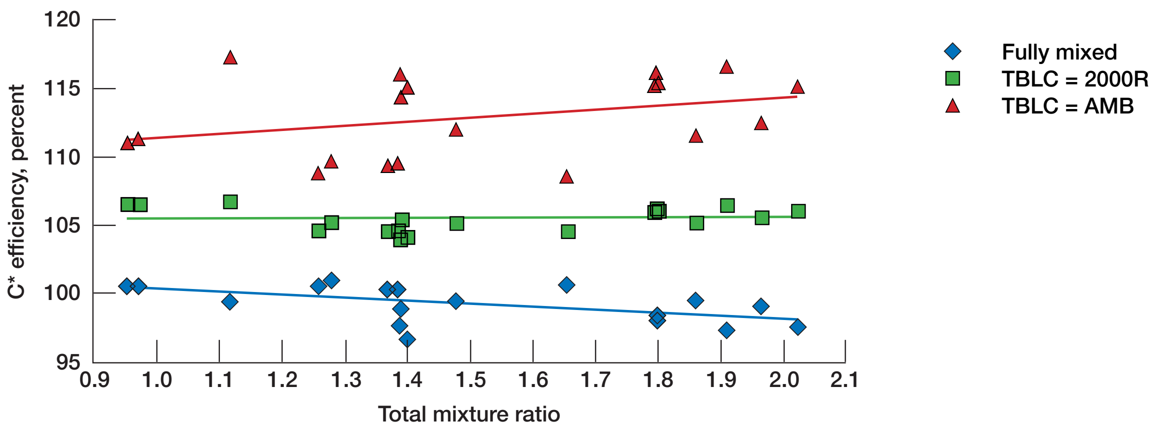

Figure 5.—C* efficiency as a function of total mixture ratio.

The results show a divergence in trends between the three methods of analysis. The fully mixed case demonstrated a decreasing trend in performance based upon total mixture ratio, while the ambient boundary layer assumption provided an increasing trend. The ambient boundary layer results have significantly more scatter than the other methods presented, which may be a bi-product of the non-physical nature of the assumption, but more likely uncertainty in the flowrate measurements. The use of a 2000 °R hydrogen boundary layer resulted in a flat trend across the mixture ratio range. Average calculated performance level decreases with increasing boundary layer temperature assumptions.

Due to the amount of scatter and lack of information regarding mixing between the boundary layer and core flow, no definite conclusion can be reached on combustion efficiency based upon the results. However, it does appear, despite the large amount of boundary layer cooling, that combustion efficiencies of greater than 97 percent are achievable.

To further examine the data, C* efficiency was plotted as a function of core injector mixture ratio, and the results are plotted in figure 6. As with total mixture ratio, the results show multiple trends in performance with an increasing injector mixture ratio. The disparity in results is more pronounced based upon this method as evident from the slopes for both the ambient boundary layer assumption and the fully mixed assumption. This indicates that scatter in the boundary layer mass flow measurement has a significant effect on the results. As with the previous method, the results from the 2000 °R boundary layer analysis are flat across the core mixture ratio range.

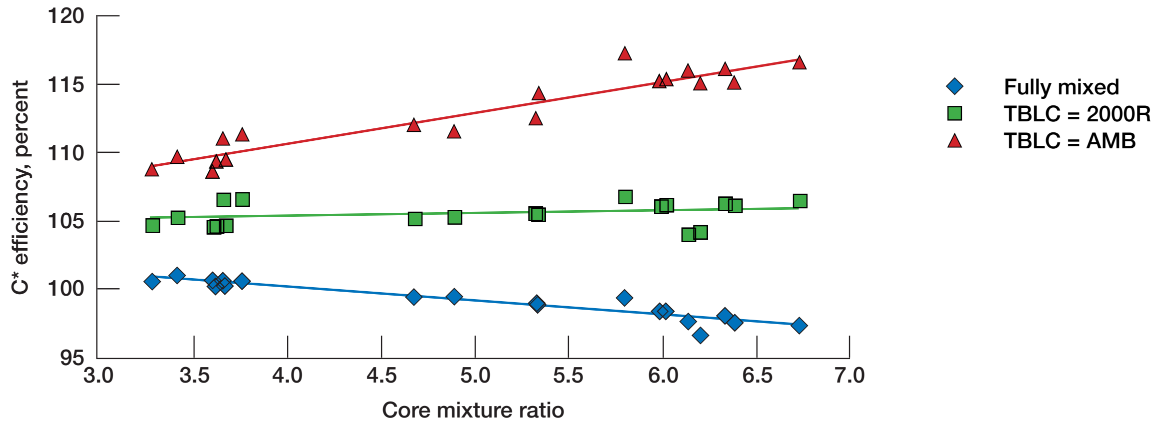

Figure 6.—C* efficiency as a function of injector core mixture ratio.

The effect on C* efficiency from the amount of boundary layer flow as a percent of the total mass flow was also examined. As shown in figure 7, a significant amount of boundary layer flow (20 to 38 percent) was used to cool the chamber walls. The results show that effects due to the percentage of boundary layer flow is relatively flat with increasing percentage. One interesting feature on the fully mixed results is that the linear curve fit of the results falls completely below the 100 percent level, whereas for the mixture ratio analysis the results showed a trend of slightly increasing performance (above 100 percent) with reduced mixture ratio.

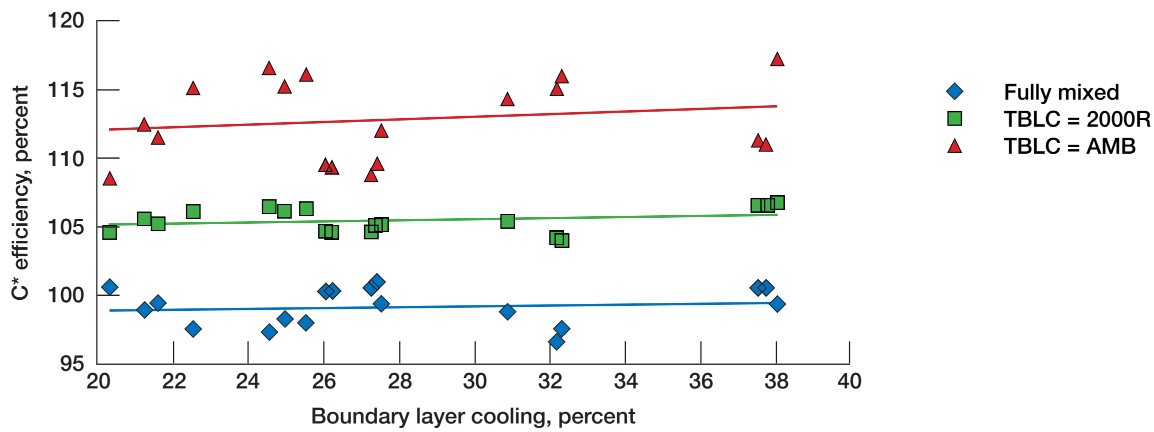

Figure 7.—C* efficiency as a function of percent boundary layer flow.

Figure 8 shows the results of C* efficiency for the fully mixed analysis again plotted against core mixture ratio. However, in this plot the data has been divided into groups based upon chamber pressure ranges of 100 psia increments from 450 to 1050 psia. The results show no effect due to chamber pressure with in the ranges of mixture ratios.

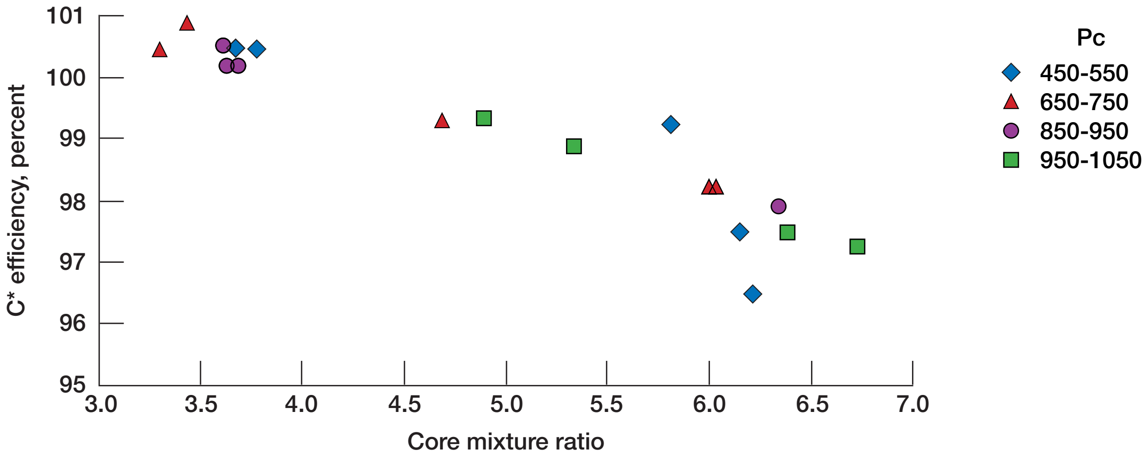

Figure 8.—C* efficiency as a function of core mixture ratio for the fully mixed analysis with data grouped by chamber pressure range.

Velocity ratio through the injector elements was also examined to determine if there was any correlation with C* efficiency. The calculation discounts any potential effects from the boundary layer flow upon performance. Velocity was calculated at the exit of the coaxial elements, before any combustion occurs. For the purposes of this study, velocity ratio was defined as:

$$VR = \frac{V_{H_2}}{V_{O_2}} \quad \textbf{(9)}$$

where the velocities were calculated by:

$$V = \frac{\dot{m}}{\rho A} \quad \textbf{(10)}$$

Velocity for the hydrogen was based on the simplifying assumption that all core hydrogen flow was injected through the elements. Density was calculated based upon measured chamber pressure and propellant inlet temperature. Results of C* efficiency as a function of velocity ratio for is plotted in figure 9 for the three methods of C* efficiency calculations. Results show the diverging trends between the various methods. Results for the fully mixed analysis are consistent with the core mixture ratio comparison of figure 6 because velocity ratio increases with a decrease in mixture ratio for the same injector element.

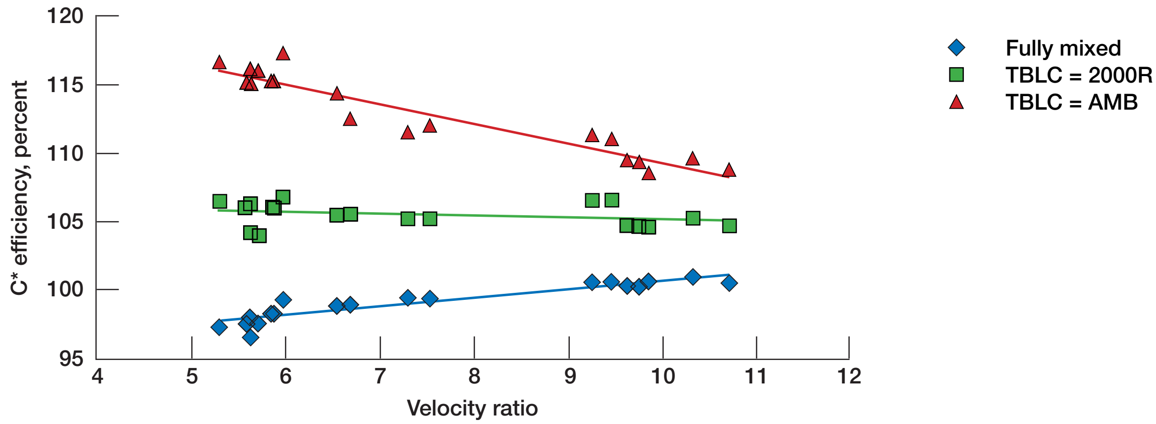

Figure 9.—C* efficiency as a function of velocity ratio.

A calculation was also performed to examine a possible correlation of performance as a function of momentum ratio, which is defined as the following.

$$MRT = \frac{\dot{m}_{H_2} * V_{H_2}}{\dot{m}_{O_2} * V_{O_2}} \tag{12}$$

As shown in figure 10, the results follow the same general trend as velocity ratio. Combustion efficiency for the fully mixed analysis increases with increasing momentum ratio.

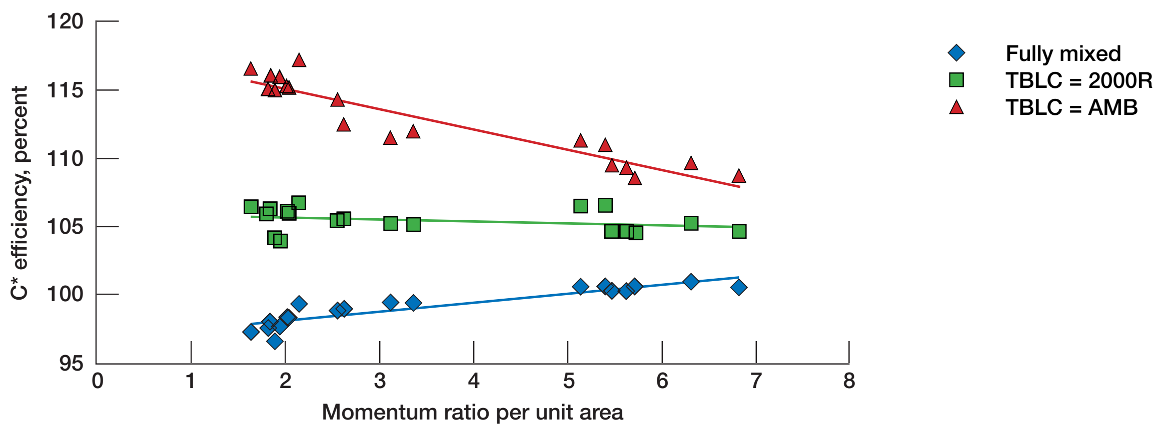

Figure 10.—C* efficiency as a function of momentum ratio.

Thermal environment

One of the key areas of interest in the development of gas-gas injectors is cooling of the injector face. To alleviate some of the cooling issues a porous metal faceplate was used to provide transpiration cooling of hydrogen through the face. In the current configuration this is a reasonable approach since the hydrogen is still relatively cool at ambient room temperature. However, in an operational system the hydrogen through the face will actually be hydrogen rich gas generator exhaust at an elevated temperature, which has significantly less cooling capacity. The current testing did not experience any significant problems with face cooling. Figures 11(a) and 11(b) show the posttest condition of the injector face. There is minimal distress on the face and the main injector elements are all in good shape. However, there was some melting on two of the face screws; while not indicative of a fundamental cooling problem, it does show the sensitivity of the issue.

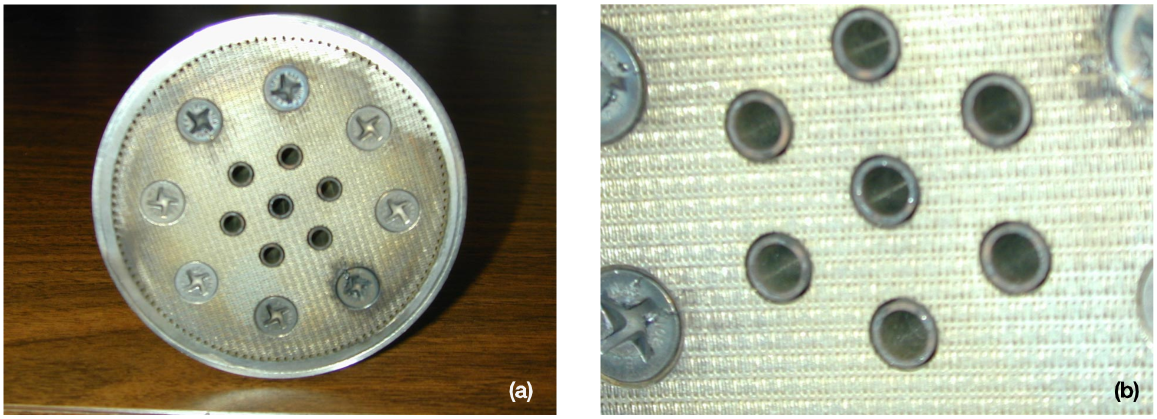

Figure 11.—Post test condition of injector face and main injection elements.

Combustion chamber wall temperature measurements were obtained at five locations along the length of the chamber. Location of the thermocouples was shown previously in figure 2 and table 2. The results shown in figures 12 to 14 give some indication of the location of combustion in the chamber. From figure 12, the thermocouples within the first 3.4 inches downstream from the injector face (TCW 1–3) are consistent, with temperatures in the range of 750 to 1100 °R. However, the two thermocouples located 5.5 inches downstream from the injector face (TCW 4 and 5), shows a temperature increase, which indicates additional heat release at that location. However, this could be due to either additional heat release from the core flow or to more complete mixing between the core and boundary layer flows. The thermocouple at TCW5 reads significantly higher in some cases, which may be an indication of combustion non-uniformity or simply that the thermocouple tip was extended into the flow farther than the others.

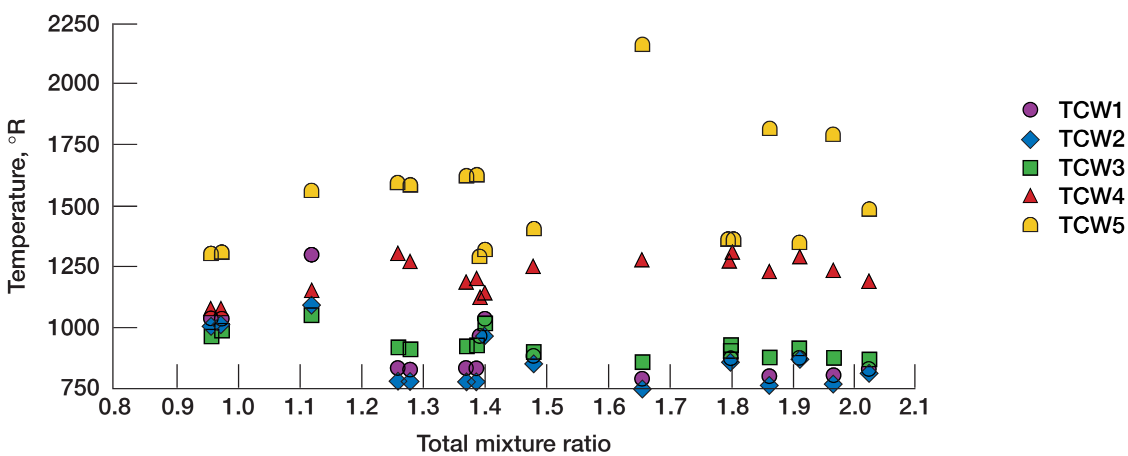

Figure 12.—Wall temperatures as a function of total mixture ratio.

The results from the total mixture ratio analysis when compared to injector mixture ratio show a consistent pattern to the temperature distribution. In most cases the thermocouple located 5.5 inches downstream of the injector face read higher than the other measurements.

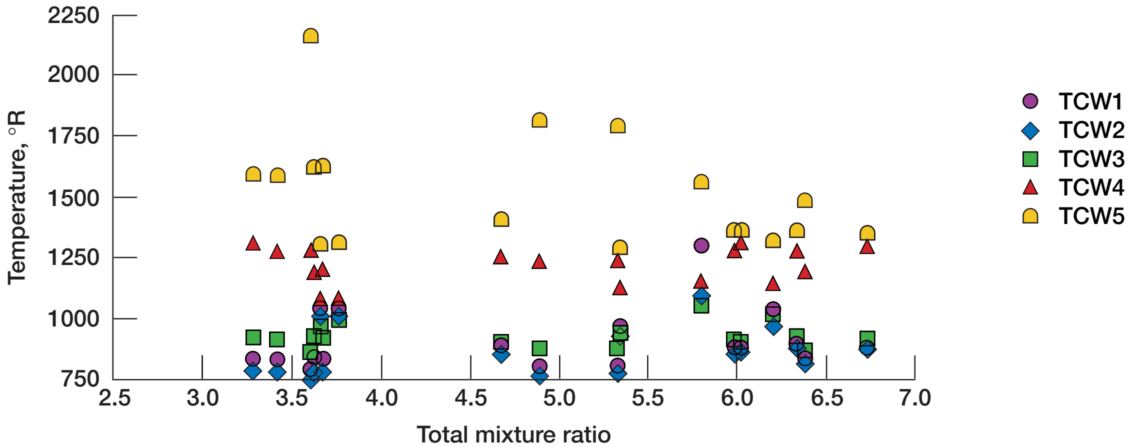

Figure 13.—Wall temperatures as a function of injector mixture ratio.

Finally, the results were plotted as a function of chamber pressure. There is no relevant trend based upon the plot, as the excess boundary layer flow was successful in reducing wall temperature through the entire test matrix.

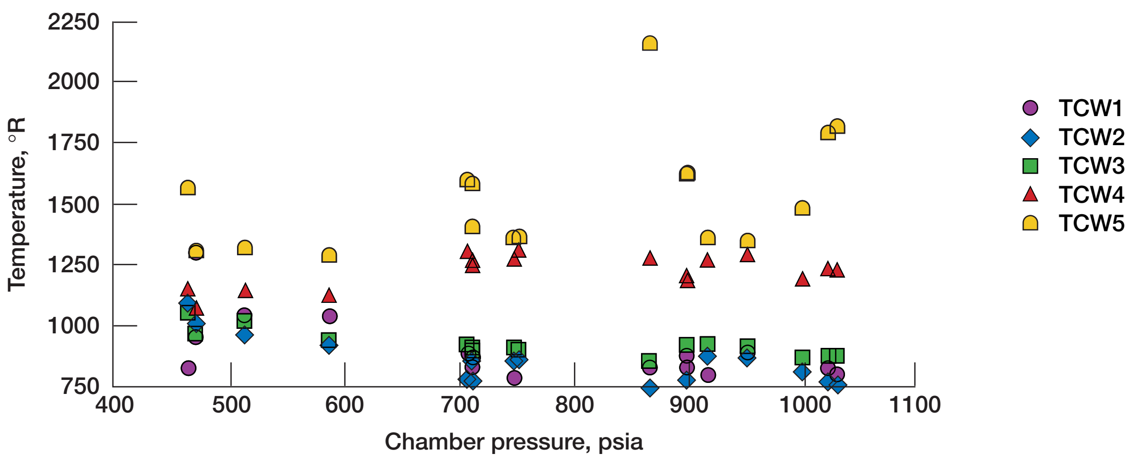

Figure 14.—Wall temperatures as a function of chamber pressure.

Summary

An experimental test program was conducted to evaluate the performance of a rocket engine injector designed for use with gaseous hydrogen and gaseous oxygen propellants. A total of 19 hot-fire tests were completed with a 7-element coaxial injector design in a heat sink combustion chamber with a 1.18-in. diameter throat. A comparison was made of the current design with the best available design correlation.

All propellants were injected at ambient temperature (529 to 555 °R). Combustion chamber walls were cooled with a layer of hydrogen injected through 120 orifices located around the injector periphery. Test firings were conducted at combustion chamber pressures of 470 to 1030 psia, total mixture ratios of 0.96 to 2.03, and injector mixture ratios of 3.3 to 6.7. The injector survived the testing with no significant discoloration or erosion to either the faceplate or oxygen posts at the conditions tested.

Injector performance was based upon calculated values for characteristic exhaust velocity (C*) efficiency. Measurements were obtained for combustion chamber pressure and mass flow. Temperature measurements were obtained at 5 locations along the length of the combustion chamber. Due to the amount of boundary layer coolant present, three methods were used to calculate C* efficiency based on fully mixed and streamtube flow. The fully mixed analysis assumed that all propellants were completely mixed to the total mixture ratio whereas the streamtube analysis assumed the boundary layer coolant did not mix with the core flow and either stayed at injection ambient temperature or was heated to 2000 °R. Unfortunately, the presence of large amounts of boundary layer flow prevented any quantitative conclusions to be obtained for injector performance. The C* efficiency range for the three methods of analysis was 97 to 117 percent, with the ambient streamtube analysis providing the high range of results and the fully mixed analysis providing the low range of results. Values greater than 100 percent for the fully mixed results can be attributed to experimental uncertainty, which was in the range of 4 to 6 percent. Values up to 117 percent for the streamtube analysis indicate that there was significant mixing between the streams. Therefore, the trends from the streamtube analysis, particularly the ambient temperature boundary layer method, are not indicative of the phenomena observed in the experiment. However, a qualitative analysis of the results can lead to the conclusion that a coaxial gas-gas injector design can provide a high level of performance based upon the fact that all performance levels were greater than 97 percent despite the significant presence of excess hydrogen. A comparison of general trends shows decreasing performance with increasing mixture ratio based upon the fully mixed analysis. However, uncertainty with the experimental results indicate that to obtain detailed performance data on specific main injector element designs, the presence of any boundary layer or secondary cooling inside the chamber should be avoided. Future testing to evaluate gas-gas injector performance should be conducted with either heat sink or actively cooled combustion chambers. Additional fidelity can be obtained by obtaining thrust measurements to corroborate results calculated from chamber pressure measurements.

References

[1] Farhangi, S., Yu, T.I., Rojas, L., Sprouse, K., and McKinnon, J.; "Gas-Gas Injector Technology for Full Flow Stage Combustion Cycle Application," AIAA 99-2757, 35th AIAA Joint Propulsion Conference, June 20–23, 1999, Los Angeles, CA

[2] Farhangi, S., Yu, T.I., Rojas, L., Sprouse, K., and Fisher, S.: "Gas-Gas Main Injector Development for Full-Flow Staged Combustion Cycle," 12th Annual PERC Symposium on Propulsion, Cleveland, OH, October 26–27, 2000.

[3] Paster, R.D.; "Hydrogen-Oxygen APS Engines," Final Report, Volume 1 and 2, Rockwell International, Rocketdyne Division, NASA CR–120805 and CR–120806, February 173.

[4] Heckert, B.J.; Yu, T.I.; Allums, S.L.; and Carrasquillo, E.A.: "25-lbf Gaseous Oxygen/Gaseous Hydrogen Thruster for Space Station Application," JANNAF Propulsion Meeting, New Orleans, LA, August 1986.

[5] Robinson, P.J.: "Space Station Auxiliary Thrust Chamber Technology," Aerojet Final Report, NASA CR–185296, July 1990.

[6] Jones, R.E.; Morren, W.E.; Sovey, J.S.; and Tacina, R.R.: "Space Station Propulsion," NASA TM–100216, 1987.

[7] Calhoon, D., Ito, J., and Kors, D., "Investigation of Gaseous Propellant Combustion and Associated Injector-Chamber Design Guidelines," Aerojet Liquid Rocket Company, NASA CR–121234, Contract NAS3–13379, July 1973.

[8] Tucker, P.K., Klem, M.D., Smith, T.D., Farhangi, S., Fisher, S.C., and Santoro, R.J.; "Design of Efficient GO2/GH2 Injectors: A NASA, Industry and University Cooperative Effort," AIAA 97–3350, 33rd AIAA Joint Propulsion Conference, July 6–9, 1997, Seattle, WA.

[9] Faust, M.J.; Deshpande, M.; Pal, S.; Ni, T.; Merkle, C.L.; and Santoro, R.J.: "Experimental and Analytical Characterization of a Shear Coaxial combusting GO2/GH2 Flowfield." AIAA 96–0646, 32ndAIAA Aerospace Sciences Meeting & Exhibit, January 15–18, 1996.

[10] Zoeckler, J.G., Green, J.I., Raitano, P. "A New Facility for Advanced Rocket Propulsion Research," NASA TM–106193, June 1993.

[11] Gordon, S.; and McBride, B.J.: Computer Program for Calculation of Complex Chemical Equilibrium Compositions and Applications. NASA RP–1311, 1994.

[12] Davidian, K.J.; Dieck, R.H.; and Chuang, I.: A Detailed Description of the Uncertainty Analysis for High Area Ratio Rocket Nozzle Tests at the NASA Lewis Research Center. 24th JANNAF Combustion Meeting, NASA TM–100203, October 1987.

REPORT DOCUMENTATION PAGE			Form Approved OMB No. 0704-0188

1. AGENCY USE ONLY (*Leave blank*)	2. REPORT DATE	3. REPORT TYPE AND DATES COVERED
	November 2002	Technical Memorandum

4. TITLE AND SUBTITLE	5. FUNDING NUMBERS
Experimental Evaluation of a Subscale Gaseous Hydrogen/Gaseous Oxygen Coaxial Rocket Injector	WU–708–73–10–00
6. AUTHOR(S) Timothy D. Smith, Mark D. Klem, Kevin J. Breisacher, Shahram Farhangi, and Robert Sutton	

7. PERFORMING ORGANIZATION NAME(S) AND ADDRESS(ES)	8. PERFORMING ORGANIZATION REPORT NUMBER
National Aeronautics and Space Administration John H. Glenn Research Center at Lewis Field Cleveland, Ohio 44135–3191	E–13652

9. SPONSORING/MONITORING AGENCY NAME(S) AND ADDRESS(ES)	10. SPONSORING/MONITORING AGENCY REPORT NUMBER
National Aeronautics and Space Administration Washington, DC 20546–0001	NASA TM—2002-211982

11. SUPPLEMENTARY NOTES

Timothy D. Smith, Mark D. Klem, and Kevin J. Breisacher, NASA Glenn Research Center; Shahram Farhangi and Robert Sutton, Boeing, Rocketdyne Division, Canoga Park, California. Responsible person, Timothy D. Smith, organization code 5830, 216–977–7546.

12a. DISTRIBUTION/AVAILABILITY STATEMENT	12b. DISTRIBUTION CODE
Unclassified - Unlimited Subject Category: 20 Distribution: Nonstandard Available electronically at http://gltrs.grc.nasa.gov This publication is available from the NASA Center for AeroSpace Information, 301–621–0390.	

13. ABSTRACT ***(Maximum 200 words)***

The next generation reusable launch vehicle may utilize a Full-Flow Stage Combustion (FFSC) rocket engine cycle. One of the key technologies required is the development of an injector that uses gaseous oxygen and gaseous hydrogen as propellants. Gas-gas propellant injection provides an engine with increased stability margin over a range of throttle set points. This paper summarizes an injector design and testing effort that evaluated a coaxial rocket injector for use with gaseous oxygen and gaseous hydrogen propellants. A total of 19 hot-fire tests were conducted up to a chamber pressure of 1030 psia, over a range of 3.3 to 6.7 for injector element mixture ratio. Post-test condition of the hardware was also used to assess injector face cooling. Results show that high combustion performance levels could be achieved with gas-gas propellants and there were no problems with excessive face heating for the conditions tested.

14. SUBJECT TERMS	15. NUMBER OF PAGES
Rocket engines; Injectors; Gaseous rocket propellants; Rocket engine design	21
	16. PRICE CODE

17. SECURITY CLASSIFICATION OF REPORT	18. SECURITY CLASSIFICATION OF THIS PAGE	19. SECURITY CLASSIFICATION OF ABSTRACT	20. LIMITATION OF ABSTRACT
Unclassified	Unclassified	Unclassified	

NSN 7540-01-280-5500

Standard Form 298 (Rev. 2-89)
Prescribed by ANSI Std. Z39-18
298-102